

## Structural and Electrical Characterization of Zinc Oxide Doped with Antimony

G. Juárez Díaz<sup>1,\*</sup>, J. Martínez-Juarez<sup>2</sup>, P. López Salazar<sup>2</sup>, R. Peña-Sierra<sup>3</sup>, J. I. Contreras-Rascon<sup>4</sup>,  
J. Díaz-Reyes<sup>5</sup>

<sup>1</sup>Facultad de Ciencias de la Computación, BUAP, Av. San Claudio y 14 Sur, Ciudad Universitaria Edificio 104, C.P. 72570, Puebla, Pue. Mexico

<sup>2</sup>Centro de Investigaciones en Dispositivos Semiconductores, BUAP, Av. San Claudio y 14 Sur, Ciudad Universitaria Edificio 103, C.P. 72570, Puebla, Pue. Mexico

<sup>3</sup>Centro de Investigación y de Estudios Avanzados del IPN, Av. IPN 2508, Col. San Pedro Zacatenco, C. P. 07360, México, D.F.

<sup>4</sup>Colegio de la Frontera Sur, ECOSUR, Carretera Panamericana y Periférico Sur s/n, Barrio María Auxiliadora, C.P. 29290, San Cristóbal de Las Casas, Chiapas, Mexico

<sup>5</sup>Centro de Investigación en Biotecnología aplicada, IPN, Ex-Hacienda San Juan Molino Carretera Estatal Tecuexcomac-Tepetitla Km 1.5, Tlaxcala C.P. 90700, Mexico

\*j.gabriel@rocketmail.com

**Abstract.** This work report on the structural and electrical characteristics of zinc oxide single crystal samples doped with antimony. Doping was carried out by antimony thermal diffusion at 1000 °C for periods of one and two hours under nitrogen environment from a solid source formed by antimony oxide. X-ray diffraction was used to determine the crystalline phases in samples and the structural change owing to diffusion. Electrical characterization by Hall effect and I-V curves showed an increase in acceptor concentration and conductivity which demonstrates that doping is effective and create acceptors in zinc oxide samples.

**Keywords:** zinc oxide; antimony doping; electrical characterization; x-ray diffraction; thermal diffusion.

### 1. Introduction

Zinc oxide (ZnO) is a semiconductor material with a direct wide band gap (3.37 eV) and large exciton binding energy (60 meV) at room temperature, this is suitable for promising applications such lasers [1], light emitting diodes [2] UV detectors [3], etc. However, it is well known that fabrication of *p*-type ZnO is rather difficult due to the self-compensating effect from native defects  $V_O$  and  $Zn_i$  and/or H incorporation.

Recently has been tried to grow *p*-type ZnO. To seek better *p*-type dopants, a few groups have tried other group-V elements, including P, As, and Sb [5], which have much larger ionic radii than oxygen atom. Surprisingly, good *p*-

type conductivities were observed from these films, indicating the feasibility of *p*-type doping with large-size-mismatched impurities [6]. Recently, Limpijumngong et al. [7] proposed a new doping mechanism for As and Sb impurities in ZnO based on a first-principles calculation. They suggested that Sb would substitute for Zn instead of oxygen and then produce two corresponding Zn vacancies, which is an  $As_{Zn}-2V_{Zn}$   $Sb_{Zn}-2V_{Zn}$  complex. However, few Sb-doped ZnO studies were reported in the literature.

In this paper, we report the structural and electrical analysis of doping with antimony in single crystal ZnO samples carried out by atomic diffusion. The crystalline phase change of doping material, introduction and modifications in host structure has been studied.

The results indicate that antimony is fully introduced in the ZnO samples, structural quality is kept, but the structure presents low dimensional changes.

## 2. Methodology

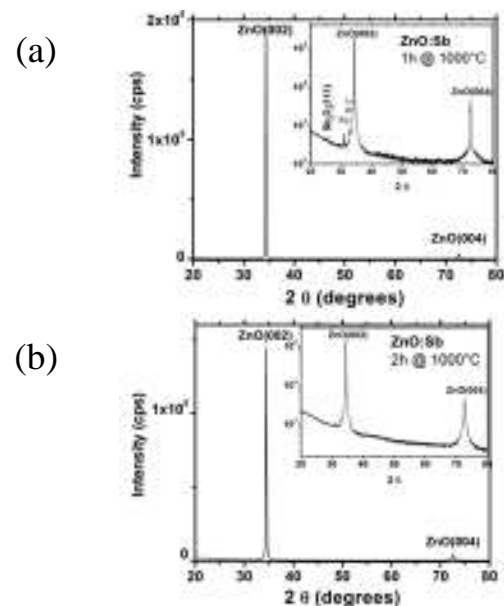
In this study, doping with antimony in single crystal ZnO was carried out by diffusion in a quartz tube furnace. A ZnO (001) single crystal substrate ( $5 \times 5 \times 0.5 \text{ mm}^3$ ) purchased from MTI crystals Co (California, USA) was used as starting material. After a standard cleaning procedure, the diffusion process consisted of three steps. In the first step, a  $1 \mu\text{m}$  elemental antimony layer was deposited on single crystal ZnO samples by evaporation of Sb (5N) in a vacuum chamber with a pressure around  $10^{-6}$  Torr. In a second step, the Sb layers were oxidized at  $300 \text{ }^\circ\text{C}$  for 1h (enough for oxidizing) under oxygen atmosphere [7]. In a third step, diffusion process was carried out in a quartz tube furnace at  $1000 \text{ }^\circ\text{C}$ , within a nitrogen ( $\text{N}_2$ ) atmosphere for periods of 1 h and 2 h.

Structural characterization for phase identification was performed by using a Bruker D8 Discover x-ray diffractometer with the  $\text{CuK}\alpha$  radiation generated at 40 kV and 40 mA, 2 theta range used in this measurement was from  $20$  to  $80^\circ$  with an increment of  $0.02^\circ$ . The crystal quality of samples was investigated using high resolution x-ray diffraction (HRXRD) in the same diffractometer with high resolution configuration that is equipped with a Goebel mirror and a V-groove compressor, producing a  $\text{CuK}\alpha 1$  radiation ( $1.5406 \text{ \AA}$ ), the measurements were made with a step of  $10^{-4}^\circ$  in a range of  $0.25^\circ$  around the (002) reflection. Reciprocal space mapping was performed using the same diffractometer to investigate the effect of antimony introduction on ZnO lattice. In order to study changes on electrical parameters due to antimony doping Hall effect measurements were performed on substrate and two samples with diffusion, using Van der Paw configuration with a magnetic field density of 0.37 Tesla, electric

contacts used were made of silver pads.

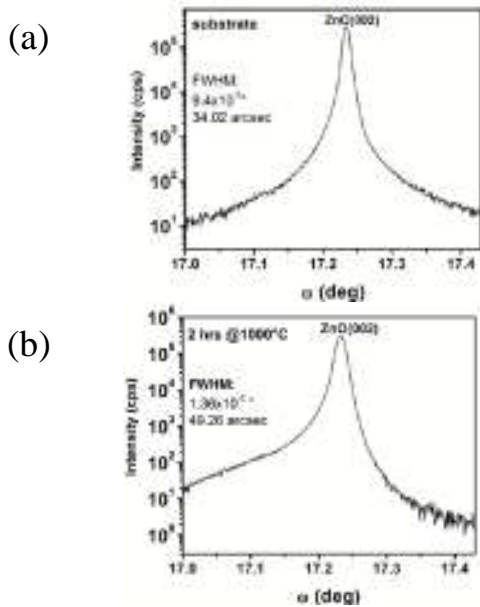
## Results and discussion

Fig. 1a shows the XRD diffractogram from the ZnO sample after a Sb diffusion of 1 h at  $1000 \text{ }^\circ\text{C}$ . Two sharp and intense peaks at  $34.4$  and  $75.6^\circ$  corresponding to (002) and (004) plane of ZnO hexagonal phase are observed, this reveals high crystallinity with the c-axis orientation normal to the sample surface. Inset in Fig. 1a shows a semi-log graph, where a peak at  $25.5^\circ$  is observed, which corresponds to  $\text{Sb}_2\text{O}_3$  orthorhombic phase (ICDD PDF 11-0689 card), also, two small peaks near the (002) reflection can be detected, these are originated by undesired  $\text{CuK}\beta$  and  $\text{WLa}$  radiation coming from anode and filament of x-ray tube, but, if these can be observed is due to high crystallinity of sample. Fig. 1b depicts the XRD pattern for sample after a Sb diffusion of 2 h at  $1000 \text{ }^\circ\text{C}$ , where the  $\text{Sb}_2\text{O}_3$  peak is not detected, this is attributed to introduction of Sb leaving the ZnO surface without  $\text{Sb}_2\text{O}_3$ , at least in an amount that is not detectable by XRD, no other diffraction peaks produced by secondary phases were observed.



**Figure 1.** XRD patterns of ZnO samples (a) after 1 h of diffusion (b) after 2 h of diffusion.

HRXRD measurements confirm that the material is preserved as single crystal material, such is observed in Fig. 2a and b where rocking curves around (002) reflection are presented. The Sb increases the full width at half maximum (FWHM) in the rocking curves of (002) reflection from 34.02 arcsec measured in substrate to 46.06 and 49.26 arcsec for 1 h and 2 h diffused samples, respectively, which means that Sb introduction modifies the lattice, probably creating tensile strain [8].



**Figure 2.** HRXRD rocking curves of ZnO samples (a) before the diffusion (b) after 2 h of diffusion.

Reciprocal space maps formed by *h* and *l* Miller indexes are presented in Fig. 3a and b for ZnO substrate and sample with 2h diffusion, respectively. Before the diffusion the intensity around the (002) reflection is focused in center of map. After 2 h of diffusion the dispersion intensity is increased and shift to lower *l* values, which indicates a low dimensional change in interplanar distance increasing stress along *c*-axis, according to relation between reciprocal and direct lattice the change in interplanar distance has a maximum value of 0.208 Å along the *c*-axis due to Sb introduced in lattice. Despite the symmetry of lattice the change in structure is higher along the *c*-axis, due probably

to direction of diffusion and the available sites for interstitial atoms.

Depth of introduction of Sb in ZnO lattice is expected has a value in the order of a few micrometers as has been measured in previous work using SIMS [9].

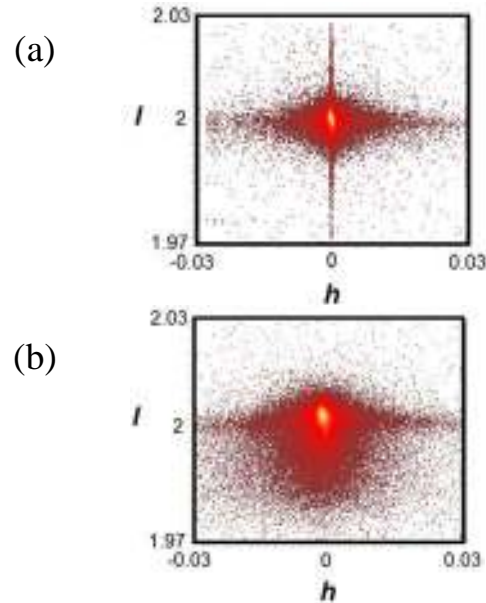


**Figure 3.** HRXRD reciprocal space maps of ZnO samples (a) before the diffusion (b) after 2 h of diffusion.

Hall effect measurements provided values of electrical parameters for ZnO substrate and samples with diffusion, these results are showed in Table I. Concentration is increased one order of magnitude and elevated as diffusion time is increased, this is attributed to the Sb atoms occupied the Zn sites and are active due to process temperature, result of this the conductivity type changes from *n* to *p*-type. Mobility is decreased as diffusion time is higher, probably due to scattering of point defects generated from substitution of Sb atoms in lattice. The conductivity value decreases one order of magnitude according to the increment in carrier concentration and probably to an improvement of ohmic contact with doped ZnO, these results indicate that antimony is effectively introduced in ZnO lattice.

The I-V characteristics for electrical properties of ZnO doped samples are shown in

**Table I.** Hall effect results for ZnO samples before and after diffusion.

Diffusion time (h)	Carrier concentration ( $\times 10^{15} \text{ cm}^{-3}$ )	Electrical parameters		
		Conductivity type	Mobility ( $\text{cm}^2/\text{V s}$ )	Conductivity ( $\times 10^{-2} \Omega \text{ cm}$ )
0*	0.361	<i>n</i>	129.07	0.748
1	5.16	<i>p</i>	38.52	2.74
2	7.25	<i>p</i>	30.78	4.79

\*Substrate

Fig. 4. The I-V measurements were acquired under dark conditions. These curves show that the electrical conductance level of the samples is influenced by antimony introduction. The conductance is increased as the diffusion time is higher, this can be observed from measured current for sample with two hour of diffusion, the value is raised for positive bias; this is attributed to a shallow *p-n* junction.

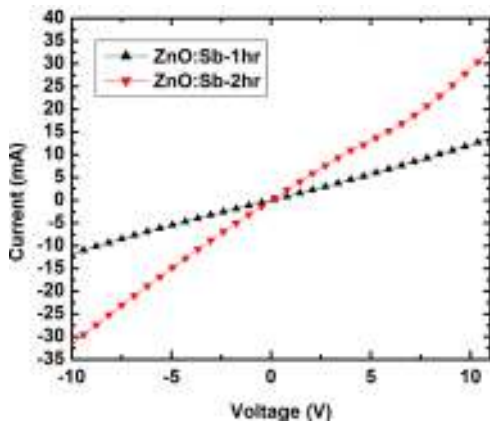


**Figure 4.** I-V Curves for ZnO samples with different periods of diffusion.

### Conclusions

Single crystal zinc oxide (001) oriented was doped with antimony by atomic diffusion at 1000 °C. The XRD measurements showed that doping source had a  $\text{Sb}_2\text{O}_3$  orthorhombic phase and after 2h of diffusion the Sb is entirely introduced and high crystallinity of ZnO is conserved. HRXRD results indicate that Sb introduction modifies the ZnO lattice increasing the FWHM of rocking curves from 34.02 to

49.26 arcsec. Reciprocal space mapping reveals that Sb diffusion modifies ZnO structure at low dimensions the correspondence with direct space the lattice is increased along *c*-axis with a maximum value of 0.208 Å. From electrical characterization can be observed that antimony modifies the carrier concentration, mobility, conductivity and I-V behavior, which indicates that antimony is effectively introduced.

### References

[1] M. H. Huang, S. Mao, H. Feick, H. Yan, Y. Wu, H. Kind, E. Weber, R. Russo, P. Yang, Room-temperature ultraviolet nanowire nanolasers, *Science* **292** (2001) 1897-1899.

[2] D. -K. Hwang, S. -H. Kang, J. -H. Lim, E. -J. Yang, J. -Y. Oh, J. -H. Yang, S. -J. Park, *p*-ZnO/*n*-GaN heterostructure ZnO light-emitting diodes, *Appl. Phys. Lett.* **86** (2005) 222101-3.

[3] A. Allenic, W. Guo, Y. B. Chen, M. B. Katz, G. Y. Zhao, Y. Che, Z. D. Hu, B. Liu, S. B. Zhang, X. Q. Pan, Amphoteric phosphorus doping for stable *p*-type ZnO, *Adv. Mater.* **19** (2007) 3333-3337.

[4] Z. Fu, W. Dong, B. Yang, Z. Wang, Y. Yang, H. Yan, S. Zhang, J. Zuo, M. Ma, X. Liu, Effect of MgO on the enhancement of ultraviolet photoluminescence in ZnO, *Solid State Commun.* **138** (2006) 179-183.

- [5] T. Aoki, Y. Shimizu, A. Miyake, A. Nakamura, Y. Nakanishi, Y. Hatanaka, *p*-type ZnO layer formation by excimer laser doping, *Physica Status Solidi B* **229** (2002) 911-914.
- [6] V. Vaithianathan, B. -T. Lee, S. S. Kim, Preparation of As-doped *p*-type ZnO films using a Zn<sub>3</sub>As<sub>2</sub> / ZnO target with pulsed laser deposition, *Appl. Phys. Lett.* **86** (2005) 062101-3.
- [7] R. G. Orman, D. Holland, Thermal phase transitions in antimony (III) oxides, *J. Solid State Chem.* **180** (2007) 2587-2596.
- [8] A. Khorsand Zak, W. H. Abd. Majid, M. E. Abrishami, R. Yousefi, X-ray analysis of ZnO nanoparticles by Williamson–Hall and size-strain plot methods, *Solid State Sci.* **13** (2011) 251.
- [9] G. Juárez Díaz (2010) *Ph.D. thesis*, CINVESTAV-Instituto Politécnico Nacional, Mexico.